

## Hexagonal BCN Films Prepared by RF Plasma-enhanced CVD

Md. Abdul Mannan,<sup>\*1</sup> Masamitsu Nagano,<sup>1</sup> Norie Hirao,<sup>2</sup> and Yuji Baba<sup>2</sup>

<sup>1</sup>Department of Applied Chemistry, Faculty of Science and Engineering, Saga University, 1 Honjo, Saga 840-8502

<sup>2</sup>Synchrotron Radiation Research Unit, Quantum Beam Science Directorate, Japan Atomic Energy Agency, Tokai-mura, Ibaraki 319-1195

(Received October 4, 2007; CL-071098; E-mail: amannan75@yahoo.com)

Hexagonal boron carbonitride (h-BCN) films have been synthesized on silicon (100) substrate by radio frequency plasma enhance chemical vapor deposition from tris(dimethylamino)-borane (TDMAB) as a precursor. XPS and FT-IR revealed that the film with a composition of  $B_{46}C_{18}N_{36}$  had  $sp^2$  B–C–N atomic hybridization. NEXAFS suggested that the local structure of BCN showed different atomic orientations to the substrate.

Recently, the boron carbonitride (BCN) films have attracted much attention due to their potential applications to electronic, optoelectronic, and luminescent devices. The cubic boron carbonitride (c-BCN) is expected to be a hard material superior to diamond and the hexagonal compound (h-BCN) is attractive in the applications to electronic devices, due to its semi-conducting properties with variable energy band-gap. It might also be applicable to the rechargeable Li battery.<sup>1</sup> Much effort has been devoted to synthesis of the ternary boron carbonitride films with different compositions.<sup>2,3</sup> However, the preparation of a single phase of the cubic or hexagonal BCN compounds is still a great challenge.

In this work, we report hexagonal BCN films synthesized on Si from TDMAB by inductively coupled radiofrequency plasma enhanced chemical vapor deposition (RF-PECVD).

The deposition was performed at the RF power of 400–900 W, at the working pressure of about 0.3 Torr, and at the  $H_2$  flow of 50 sccm. The chemical binding state and composition of the deposited films were investigated by FT-IR, XPS, and NEXAFS. The XPS and NEXAFS measurements were performed at the Beam Line 27A and Beam Line 11A of the Photon Factory in the High Energy Acceleration Research Organization (KEK-PF), using the linearly polarized synchrotron radiation. The B1s, C1s, and N1s binding energies were calibrated by  $Au4f_{7/2}$  binding energy (84.0 eV). The XPS was measured after  $Ar^+$  ion etching for 1 min.

FT-IR transmission spectrum of the typical sample showed two peaks (Figure 1); a strong and broad peak at  $1380\text{ cm}^{-1}$  and a relatively weak peak at  $800\text{ cm}^{-1}$ . These peaks are usually assigned to the hexagonal BN (h-BN).<sup>4</sup> The C–N, C=N, and C≡N bonds mostly appear approximately at 1300, 1600, and  $2170\text{ cm}^{-1}$  respectively.<sup>5</sup> The strong peak from  $1300\text{--}1600\text{ cm}^{-1}$  suggests the formation of the C–N and/or C=N bonds whilst the C≡N bonds are not confirmed. The peak also indicates incorporation of C into the h-BN to form the B–C–N hybrid compounds<sup>6</sup> and/or the complex composition from the h-BN to graphite. Concentration of carbon, estimated from XPS, was found to be 18 atom % as shown (Figure 2a). Therefore, FT-IR suggests the formation of the hexagonal BCN (h-BCN) although the phase could not be confirmed by XRD.

The wide full-width at half maximum of the B1s peak

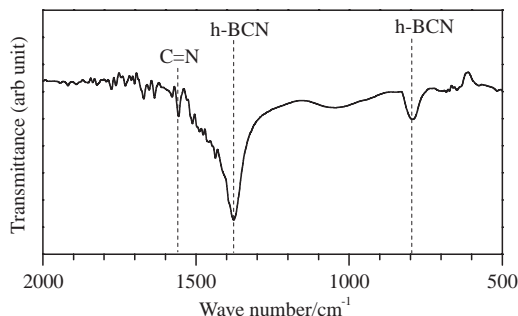


**Figure 1.** FT-IR transmission spectrum of the typical sample synthesized at RF power of 800 W, at  $750^\circ\text{C}$ , and at TDMAB flow of 1 sccm.

(>2.0 eV) (Figure 2a) compared with that of the pure h-BN (ca 1.0 eV) suggests that B atoms have various chemical environments.<sup>7</sup> The B1s spectra could be well fitted by deconvoluting into two Gaussian peaks. The dominating peak centered at 190.8 eV could be assigned to the B–N bonds in h-BN. The reported value of B1s binding energy for h-BN is distributed in the range of 189–191 eV.<sup>7</sup> The observed binding energy is located in the reported range, suggesting that B atoms in the BCN films are mainly bonded to nitrogen as  $sp^2$  B–N bonds. The B1s binding energies for  $BC_{3.4}$  and  $B_4C$  have been found to be 189.4 and 188.4 eV, respectively.<sup>8</sup> Therefore, the component peak centered at 189.6 eV could be ascribed to the  $sp^2$  B–C–N hybrid bondings. The B–C–N bondings around B atoms could be ascribed as  $BN_3$ ,  $BN_2C$ ,  $BNC_2$ , and  $BC_3$  which were schematically shown (Figure 3). The impurity oxygen was found to be less than 3 atom %.

The C1s spectra could be fitted into two peaks (Figure 2b). The dominating peak centered at 283.4 eV suggests the formation of the C–B bond.<sup>8</sup> The component peak centered at 285.1 eV is due to C atom bonded to more electronegative N atom.<sup>6</sup> These results confirm that C atoms are mostly bonded to B to form the C–B bonds although there are C atoms bonded to N to form the C–N bonds in the films.

Deconvolution of N1s revealed the presence of two possible states (Figure 2c). The component peak centered at 397.6 eV could be assigned to the N–B bond.<sup>8</sup> The N–B bonds are predominant in accordance with the fact suggested by the B1s spectra. The peak at the higher energy is originated from the N–C bond because the N–C bond has been reported to be around 398.4–400 eV.<sup>9</sup> The XPS results confirmed the formation of different B–C–N hybrid bonds.

Almost similar  $\pi^*$  resonance peak to that of the h-BN have been predominantly observed at the normal incidence ( $\theta = 0^\circ$ ) (Figure 4).

The dominating peak  $B_2$ , slightly broader than that of the

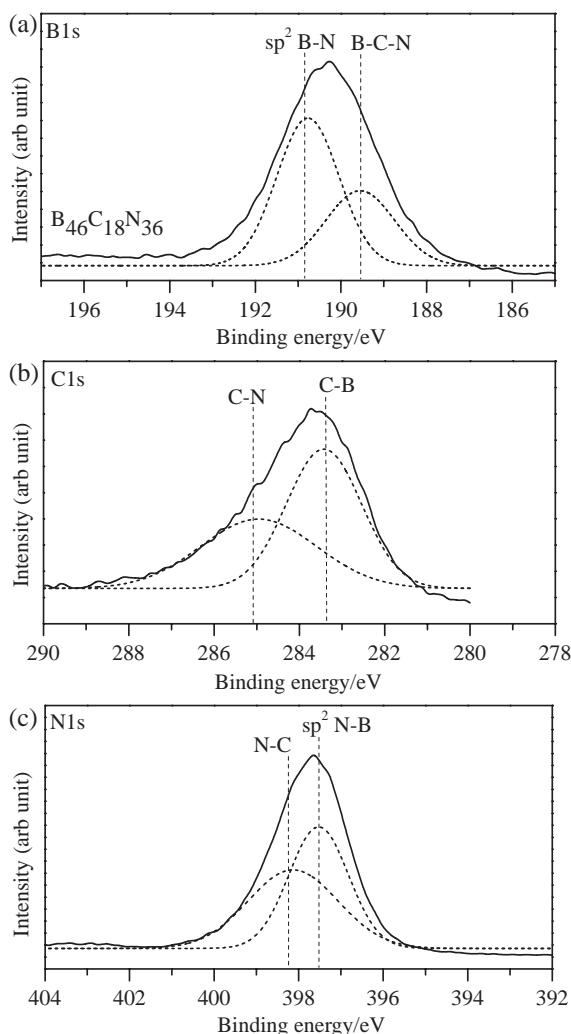


**Figure 2.** B1s, C1s, and N1s XPS spectra of the sample shown in Figure 1.

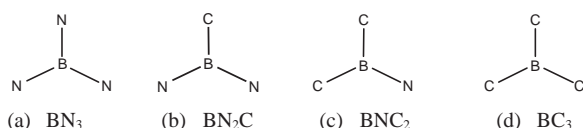


**Figure 3.** Possible  $sp^2$  bondings around B atoms in the BCN films.

h-BN, is assigned to the B–C–N bonds, suggesting the formation of BCN with a similar configuration to  $BN_3$  in h-BN. The comparatively sharp NEXAFS spectrum of the sample implies the formation of the good homogeneity in configuration as the h-BN.

As the grazing incidence was increased ( $\theta = 75^\circ$ ), the peak  $B_2$  decreased and some other peaks such as  $B_1$ ,  $B_3$ , and  $B_4$  appeared clearer. It indicates the formation of various atomic configurations around B atoms besides  $BN_3$ . The peak  $B_1$  could be ascribed to the B atoms in the  $B_4C$ -like configuration.<sup>10</sup> Peak  $B_3$  is assigned to the B atom bonded to nitrogen atoms such as  $BN_2C$ ,  $BNC_2$  as shown (Figure 3). Peak  $B_4$  is reported to be the B–O bond.<sup>11</sup> The notable decrease in  $\pi^*$  resonance peak and increase in the  $\sigma^*$  resonance peak (broad feature denoted by  $B_5$ ) with the grazing incidence suggests that different  $sp^2$  bonded BCN layers

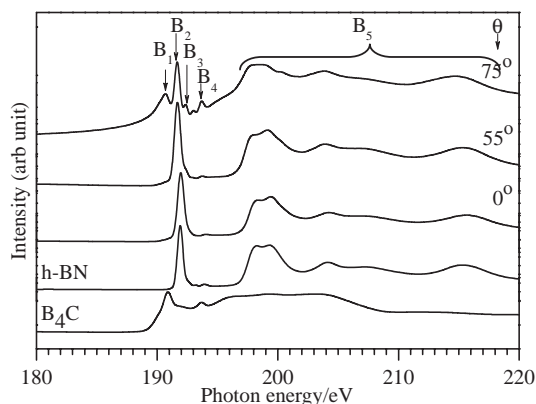


**Figure 4.** B K-edge NEXAFS spectra at various incidence angle ( $\theta$ ) of X-ray for BCN film shown in Figure 1. NEXAFS spectra for the h-BN and  $B_4C$  power are also shown for comparison.

may be perpendicular to the substrate.<sup>12</sup>

In conclusion, the formation of the hexagonal BCN using tris(dimethylamino)borane by RF-PECVD was confirmed by FT-IR. The XPS measurement revealed various B–N, B–C, and C–N bonds to form BCN atomic hybrids. It was also found from NEXAFS measurement that the h-BCN layer consisted of different configurations around the B, C, and N atoms which had the single phase of graphite-like BCN configuration although the hexagonal structure appeared in a short range order.

We would like to thank Dr. Y. Kitajima of the Photon Factory for his supports. This work was performed under the approval of the Photon Factory Program Advisory Committee (Proposal No. 2006G312).

## References

- 1 M. Kawaguchi, *Adv. Mater.* **1997**, 9, 615.
- 2 W. J. Pan, J. Sun, H. Ling, N. Xu, Z. F. Ying, J. D. Wu, *Appl. Surf. Sci.* **2003**, 218, 298.
- 3 H. Sun, S.-H. Jhi, D. Roundy, M. L. Chohen, S. G. Louie, *Phys. Rev. B* **2001**, 64, 94108.
- 4 Y. Wada, Y. K. Yap, M. Yoshimura, Y. Mori, T. Sasaki, *Diamond. Relat. Mater.* **2000**, 9, 620.
- 5 H. S. Kim, I. H. Choi, Y.-J. Baik, *Surf. Coat. Technol.* **2000**, 133–134, 473.
- 6 V. Linss, S. E. Rodil, P. Reinke, M. G. Garnier, P. Oelhafen, U. Kreissig, F. Richte, *Thin Solid Films* **2004**, 467, 76.
- 7 M. N. Uddin, I. Shimoyama, Y. Baba, T. Sekiguchi, M. Nagano, *J. Vac. Sci. Technol., A* **2005**, 23, 497.
- 8 N. Laidani, M. Anderle, R. Canteri, L. Elia, A. Luches, M. Martino, V. Micheli, G. Speranza, *Appl. Surf. Sci.* **2000**, 157, 135.
- 9 I. Shimoyama, G. Wu, T. Sekiguchi, Y. Baba, *J. Electron. Spectrosc. Relat. Phenom.* **2001**, 114–116, 841.
- 10 R. Gago, I. Jiménez, I. García, J. M. Albella, *Vacuum* **2002**, 64, 199.
- 11 S. C. Ray, H. M. Tsai, J. W. Chiou, J. C. Jan, K. Kumar, W. F. Pong, F. Z. Chien, M.-H. Tsai, S. Chattopadhyay, L. C. Chen, S. C. Chien, M. T. Lee, S. T. Lin, K. H. Chen, *Diamond Relat. Mater.* **2004**, 13, 1553.
- 12 R. Gago, I. Jiménez, T. Sajavaara, E. Hauhalo, J. M. Albella, *Diamond Relat. Mater.* **2001**, 10, 1165.